

# Selective Electrocatalytic Oxidation of a Re–Methyl Complex to Methanol by a Surface-Bound Ru<sup>II</sup> Polypyridyl Catalyst

Michael K. Coggins,<sup>†</sup> Manuel A. Méndez,<sup>†</sup> Javier J. Concepcion,<sup>†</sup> Roy A. Periana,<sup>‡</sup> and Thomas J. Meyer<sup>\*†</sup>

<sup>†</sup>Department of Chemistry, University of North Carolina at Chapel Hill, Chapel Hill, North Carolina 27599, United States

<sup>‡</sup>The Scripps Energy and Materials Center, Department of Chemistry, The Scripps Research Institute, Jupiter, Florida 33458, United States

**S** Supporting Information

**ABSTRACT:** The complex [Ru(Mebimpy)(4,4'-((HO)<sub>2</sub>OPCH<sub>2</sub>)<sub>2</sub>bpy)(OH<sub>2</sub>)]<sup>2+</sup> surface bound to tin-doped indium oxide mesoporous nanoparticle film electrodes (nanoITO-Ru<sup>II</sup>(OH<sub>2</sub>)<sup>2+</sup>) is an electrocatalyst for the selective oxidation of methylrhenium trioxide (MTO) to methanol in acidic aqueous solution. Oxidative activation of the catalyst to nanoITO-Ru<sup>IV</sup>(OH)<sup>3+</sup> induces oxidation of MTO. The reaction is first order in MTO with rate saturation observed at [MTO] > 12 mM with a limiting rate constant of  $k = 25 \text{ s}^{-1}$ . Methanol is formed selectively in 87% Faradaic yield in controlled potential electrolyses at 1.3 V vs NHE. At higher potentials, oxidation of MTO by nanoITO-Ru<sup>V</sup>(O)<sup>3+</sup> leads to multiple electrolysis products. The results of an electrochemical kinetics study point to a mechanism in which surface oxidation to nanoITO-Ru<sup>IV</sup>(OH)<sup>3+</sup> is followed by direct insertion into the rhenium–methyl bond of MTO with a detectable intermediate.

The oxidative functionalization of hydrocarbons is a fundamental chemical transformation that is of great interest in the petrochemical industry, with particular interest in the direct conversion of methane to methanol.<sup>1</sup> The absence of an industrial scale technology for this conversion is a reflection of a fundamental difficulty in the activation and subsequent functionalization of relatively inert C–H bonds.<sup>2</sup> New catalysts are needed to promote this reaction at reasonable rates under mild conditions.

Significant progress has been made with soluble transition-metal complexes as homogeneous catalysts for methane activation.<sup>3</sup> Methane hydroxylation catalysis based on electrophilic late transition-metal complexes of Hg<sup>II</sup>, Pt<sup>II</sup>, Pd<sup>II</sup>, and Au<sup>III</sup> has been documented.<sup>3</sup> These reactions require elevated temperatures and strongly acidic solutions, in some cases with stoichiometric consumption of expensive oxidants such as Pt<sup>IV</sup>.<sup>3</sup> Methane C–H bond activation has not been reported with these catalysts under milder conditions, although functionalization of metal–alkyls (M–R) has.<sup>3</sup> C–H bond activation has been reported for transition-metal complexes of Ru<sup>II</sup>, Ir<sup>I</sup>, Ir<sup>III</sup>, and Os<sup>II</sup> but without further M–R bond functionalization of the alkyl product.<sup>4</sup>

Methane hydroxylation by late transition-metal catalysts, including an initial report on Pt<sup>II</sup> salts by Shilov,<sup>3a,b</sup> has been

proposed to occur by initial C–H bond activation to give a metal–alkyl intermediate.<sup>3</sup> Subsequent oxidation of the metal–alkyl intermediate,  $M^n-R \xrightarrow{-2e^-} M^{(n+2)}-R$ , followed by nucleophilic addition of water to the  $M^{(n+2)}-R$  alkyl with dissociation of R–OH was proposed to complete the oxidation cycle.<sup>3a</sup> Direct insertion of an oxygen atom into a M–R bond to give M–OR, which avoids a change in oxidation state at the metal, has also been reported.<sup>4–6</sup> Only a handful of these reactions are known, including the migratory insertion of oxo ligands<sup>4a</sup> and oxygen atom transfer from N<sub>2</sub>O.<sup>5</sup> In recent studies, oxygen atom transfer from pyridine N-oxide, periodate, iodosylbenzene, and hydrogen peroxide has been shown to occur by direct insertion into the Re–CH<sub>3</sub> bond of methylrhenium trioxide (H<sub>3</sub>C–Re(O)<sub>3</sub>, MTO), through a pathway similar to the Baeyer–Villiger reaction, with methanol as the product in near quantitative yields.<sup>4d,f,6</sup> Catalytic oxygen atom insertion into the Re–C bond of MTO to give methanol has been demonstrated with flavins as catalysts and hydrogen peroxide as a stoichiometric oxidant.<sup>7</sup> The full scope of this reactivity and its viability as a methane to methanol conversion strategy remains to be explored in detail.

Here we report that the known water and hydrocarbon oxidation catalyst [Ru(Mebimpy)(4,4'-((HO)<sub>2</sub>OPCH<sub>2</sub>)<sub>2</sub>bpy)(OH<sub>2</sub>)]<sup>2+</sup> (**1**, Mebimpy is 2,6(1-methylbenzimidazol-2-yl) and 4,4'-((HO)<sub>2</sub>OPCH<sub>2</sub>)<sub>2</sub>bpy is 4,4'-bismethylenephosphonato-2,2'-bipyridine)<sup>8</sup> immobilized on mesoporous tin-doped indium oxide nanoparticle electrodes (nanoITO-Ru<sup>II</sup>(OH<sub>2</sub>)<sup>2+</sup>) is an electrocatalyst for the selective oxidation of MTO to methanol at pH 1.0. Results from cyclic voltammetry (CV), chronoamperometry, and controlled potential electrolysis (CPE) point to the -Ru<sup>IV</sup>(OH)<sup>3+</sup> form of **1** as the catalytically active intermediate in the selective oxidation of MTO to methanol with no competitive catalytic water oxidation, which contrasts with the higher oxidation state -Ru<sup>V</sup>(O) form of **1**.<sup>8a–c</sup> The contrast in reactivity between the two oxidation states of the same catalyst highlights an advantage of electrocatalysis over chemical catalysis by the judicious control of applied potentials to control selective oxidation.

Catalyst **1** and high surface area nanoITO electrodes (2.5 μm films of 40 nm diameter ITO nanoparticles) were prepared and characterized by known procedures.<sup>8a,9</sup> Covalent attachment of

Received: August 4, 2014

**1** to nanoITO to give nanoITO-Ru<sup>II</sup>(OH<sub>2</sub>)<sup>2+</sup> (Figure 1) was performed by soaking electrodes in a 0.25 mM loading solution

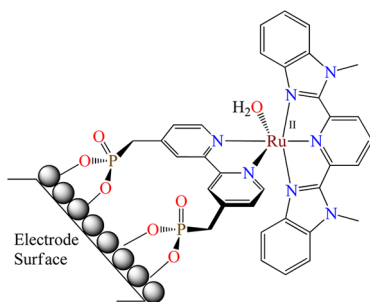


**Figure 1.** Structure of nanoITO-Ru<sup>II</sup>(OH<sub>2</sub>)<sup>2+</sup>,<sup>8,9</sup>

of **1** in 0.1 M HClO<sub>4</sub> for 12–14 h. The procedure gave fully loaded electrodes with a surface coverage ( $\Gamma$ ) of  $1 \times 10^{-8}$  mol/cm<sup>2</sup>.<sup>9</sup> At pH 1.0, nanoITO-Ru<sup>II</sup>(OH<sub>2</sub>)<sup>2+</sup> is electrochemically oxidized in a stepwise fashion through the series Ru<sup>II</sup>(OH<sub>2</sub>)<sup>2+</sup> → Ru<sup>III</sup>(OH<sub>2</sub>)<sup>3+</sup> → Ru<sup>IV</sup>(OH)<sup>3+</sup> → Ru<sup>V</sup>(O)<sup>3+</sup> with the last two steps occurring by proton-coupled electron transfer.<sup>8,9</sup> Upon oxidation of Ru<sup>IV</sup>(OH)<sup>3+</sup> ( $pK_a \sim 3$ ) to Ru<sup>V</sup>(O)<sup>3+</sup>, **1** enters a catalytic cycle for water oxidation both in solution and on oxide surfaces with an onset potential of  $\sim 1.5$  V vs NHE.<sup>9</sup> The intermediates that appear in the oxidative activation of **1**, Ru<sup>IV</sup>(OH)<sup>3+</sup>, Ru<sup>IV</sup>(O)<sup>2+</sup>, Ru<sup>V</sup>(O)<sup>3+</sup>, Ru<sup>V</sup>(O<sub>2</sub>)<sup>3+</sup>, have been shown to be capable of promoting the catalytic oxidation of benzyl alcohol and alkyl aromatics.<sup>8d,e,g</sup>

A representative CV of nanoITO-Ru<sup>II</sup>(OH<sub>2</sub>)<sup>2+</sup> at pH 1.0 (0.1 M HClO<sub>4</sub>, 0.4 M LiClO<sub>4</sub>) is shown in Figure S-1. In the CV, fully reversible waves appear for the nanoITO-Ru<sup>III</sup>(OH<sub>2</sub>)<sup>3+</sup>/Ru<sup>II</sup>(OH<sub>2</sub>)<sup>2+</sup> couple at  $E_{1/2} = 820 \pm 20$  mV vs NHE and the nanoITO-Ru<sup>IV</sup>(OH)<sup>3+</sup>/Ru<sup>III</sup>(OH<sub>2</sub>)<sup>3+</sup> couple at  $E_{1/2} = 1.32$  V vs NHE. As shown in Figure 2, the addition of MTO causes an

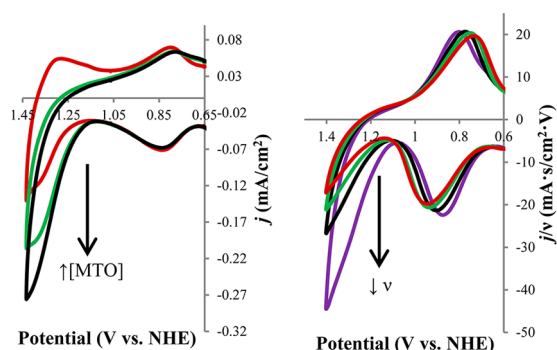


**Figure 2.** Cyclic voltammograms of nanoITO-Ru<sup>II</sup>(OH<sub>2</sub>)<sup>2+</sup> ( $\Gamma = 1 \times 10^{-8}$  mol/cm<sup>2</sup>) at pH 1.0 (0.1 M HClO<sub>4</sub>, 0.4 M LiClO<sub>4</sub>) and 10 mV/s with increasing concentrations of methylrhenum trioxide (0 mM, red; 4 mM, green; 7 mM, blue) (left). Scan-rate normalized cyclic voltammograms of nanoITO-Ru<sup>II</sup>(OH<sub>2</sub>)<sup>2+</sup> at pH 1.0 with 1.2 mM methylrhenum trioxide (50 mV/s, red; 40 mV/s, green; 25 mV/s, black; 10 mV/s, purple) (right).

increase in oxidative current density ( $j$ ) at potentials near the nanoITO-Ru<sup>IV</sup>(OH)<sup>3+</sup>/Ru<sup>III</sup>(OH<sub>2</sub>)<sup>3+</sup> couple. By contrast, there are negligible enhancements for the nanoITO-Ru<sup>III/II</sup>(OH<sub>2</sub>)<sup>3+/2+</sup> couple with added MTO (Figure 2).

MTO is redox-inactive between 0 and 1.7 V vs NHE. Additional evidence for a reaction between MTO and nanoITO-Ru<sup>IV</sup>(OH)<sup>3+</sup> appears in the scan rate normalized

CVs in Figure 2 (right) and the appearance of a scan rate dependence at slow scan rates.<sup>10</sup> CV scans were limited to potentials below  $\sim 1.4$  V due to the onset of catalytic water oxidation.<sup>8</sup> The presence or absence of O<sub>2</sub> in the external solution had no effect on the CV response. This is an important result in suggesting that the reaction between nanoITO-Ru<sup>IV</sup>(OH)<sup>3+</sup> and MTO likely does not involve intermediate radicals which react rapidly with O<sub>2</sub> under these conditions.<sup>11</sup> Radical trapping and intermediate peroxide formation would be expected to influence reaction kinetics and the product distributions (*vide infra*).<sup>11</sup>

Controlled potential electrolysis (CPE) measurements were made using fully loaded electrodes and 20 mM MTO in a closed, deoxygenated three-compartment electrolysis cell in D<sub>2</sub>O (0.1 M DClO<sub>4</sub>, 0.4 M LiClO<sub>4</sub>). D<sub>2</sub>O was used as the solvent to enable the use of <sup>1</sup>H NMR spectroscopy for product analysis. Steady-state current densities of  $\sim 0.3$  mA/cm<sup>2</sup> were maintained at an applied potential of 1.3 V vs NHE for 5 h (Figure S-2). Analysis of the electrolyte mixture by <sup>1</sup>H NMR spectroscopy after 5 h of electrolysis revealed the presence of methanol (24  $\mu$ mol) in 87% Faradaic yield (Figure S-3) with no overoxidation products, such as formic acid. Sampling of the reaction headspace and analysis by gas chromatography–mass spectrometry (GC-MS) provided no evidence for either CO or CO<sub>2</sub>. The electrolysis product distribution and yield were independent of the presence or absence of dioxygen, providing additional evidence for a nonradical mechanism.<sup>11</sup> There was no evidence for a reaction between surface-bound **1** and MTO in the absence of an applied bias. CVs of the surface-bound catalyst before and after CPE were essentially identical, thus indicating that no significant change or loss of catalyst from the electrode surface had occurred during electrolysis.

Increasing the applied potential to 1.4 V vs NHE results in steady-state current densities of  $\sim 0.5$  mA/cm<sup>2</sup> over 5 h electrolysis periods. Under these conditions there was a wide distribution of products with methanol (21  $\mu$ mol, 44% Faradaic yield), formic acid (6  $\mu$ mol, 35% Faradaic yield), and carbon dioxide (6  $\mu$ mol, 13% Faradaic yield) all appearing with a total Faradaic yield of 92% (Figures S-4,5). CPE experiments at 1.5 V vs NHE, near the anodic peak potential for the nanoITO-Ru<sup>IV</sup>(OH)<sup>3+</sup>/Ru<sup>V</sup>(O)<sup>3+</sup> couple at  $E_{p,a} \sim 1.50$  V, gave higher quantities of these same products. The appearance of multiple products at 1.40 V results from the small fraction of catalyst present as nanoITO-Ru<sup>V</sup>(O)<sup>3+</sup>. At 1.4 V, with  $E^0 \approx E_{p,a}$  for the nanoITO-Ru<sup>IV</sup>(OH)<sup>3+</sup>/Ru<sup>V</sup>(O)<sup>3+</sup> couple, the nanoITO-Ru<sup>IV</sup>(OH)<sup>3+</sup>/Ru<sup>V</sup>(O)<sup>3+</sup> ratio on the electrode surface is  $\sim 2.0 \times 10^{-2}$  from the Nernst equation with  $E^0 - E_{app} = -0.059 \log K_{eq}$ . The ability of nanoITO-Ru<sup>V</sup>(O)<sup>3+</sup> to directly oxidize methanol to formic acid and carbon dioxide was confirmed from CPE experiments with fully loaded electrodes at pH 1.0 (0.1 M HClO<sub>4</sub>, 0.4 M LiClO<sub>4</sub>) and an applied potential of 1.50 V vs NHE with 10 mM methanol and no MTO.

nanoITO-Ru<sup>V</sup>(O)<sup>3+</sup> is a known water oxidation catalyst with water oxidation occurring by O–O bond formation and involving Ru-peroxide intermediates.<sup>8</sup> The high Faradaic yields for oxidation of MTO show that water oxidation is not a major competitor under the conditions of the electrolyses.

Surface kinetics for MTO oxidation by nanoITO-Ru<sup>IV</sup>(OH)<sup>3+</sup> were investigated by chronoamperometry at pH 1.0 (0.1 M HClO<sub>4</sub>, 0.4 M LiClO<sub>4</sub>) at 1.3 V vs NHE as a function of added MTO (Figure S-6). The data were analyzed by eq 1. In this equation  $i_{cat}$  is the steady-state catalytic current,  $n_{cat}$  ( $2e^-$ ) is the electron stoichiometry for oxidation of MTO to

methanol,  $F$  is the Faraday constant,  $A$  is the area of the electrode film,  $\Gamma$  is the surface coverage, and  $k_{\text{obs}}$  is the catalytic rate constant in  $\text{s}^{-1}$ .

$$i_{\text{cat}} = n_{\text{cat}} F A \Gamma k_{\text{obs}} \quad (1)$$

As shown in Figure 3,  $k_{\text{obs}}$  is dependent on the MTO concentration, saturating with a maximum value of  $\sim 25 \text{ s}^{-1}$

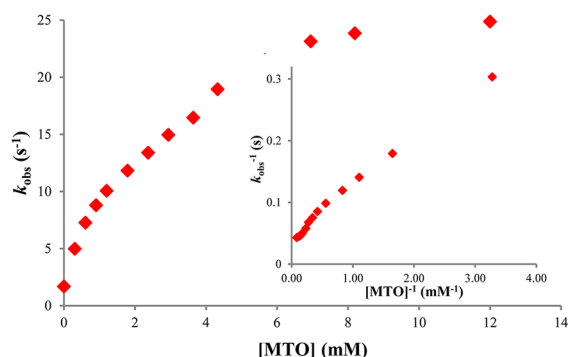


**Figure 3.** Plot of electrochemically derived rate constant for methylrhenium trioxide oxidation ( $k_{\text{obs}}$ ) on methylrhenium trioxide concentration ( $[\text{MTO}]$ , from 0.1 to 12.2 mM) from chronoamperometric measurements at pH 1.0 (0.1 M  $\text{HClO}_4$ , 0.4 M  $\text{LiClO}_4$ ) at an applied potential of 1.3 V vs NHE for nanoITO- $\text{Ru}^{\text{II}}(\text{OH})_2^{2+}$  with  $\Gamma = 1 \times 10^{-8} \text{ mol/cm}^2$ . A plot of  $k_{\text{obs}}^{-1}$  versus  $[\text{MTO}]^{-1}$  is shown in the inset.

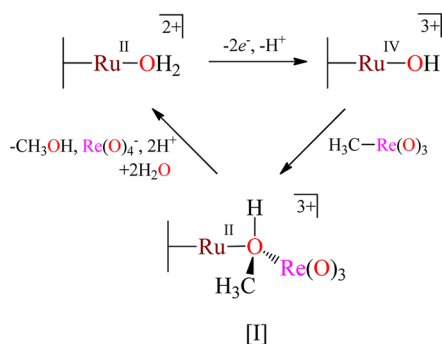
reached at  $[\text{MTO}] > 12 \text{ mM}$  at 1.3 V. Notably, the kinetics were independent of added methanol up to 50 mM consistent with the selectivity of nanoITO- $\text{Ru}^{\text{IV}}(\text{OH})_3^{3+}$  oxidation of MTO without further oxidation of methanol once it is formed. Steady-state current densities were independent of the external solution stirring rate with the length of time needed to obtain such currents varying inversely with the stirring rate (Figures S-2, 6).<sup>10</sup> The appearance of saturation kinetics at high  $[\text{MTO}]$  may signal rate-limiting diffusion of MTO into the nanoporous films, a change in rate-limiting behavior, or a combination of the two. There is evidence from spectroelectrochemical measurements, Figure S-7, for the accumulation of an intermediate in the reaction that is consistent with the observed rate saturation at high substrate concentration.

Oxidation of MTO occurs with a very small H/D solvent kinetic isotope effect (1.05) as shown by the CV comparisons in Figure S-8 and chronoamperometry experiments with  $[\text{MTO}]$  varied from 0.1 to 15 mM at pH 1.0 (0.1 M  $\text{DClO}_4$ , 0.4 M  $\text{LiClO}_4$ ). This result is consistent with a rate-limiting step or steps in which there is no significant proton involvement.

Chronoamperometry experiments were conducted with both fully loaded ( $\Gamma = 1 \times 10^{-8} \text{ mol/cm}^2$ ) and partly loaded ( $\Gamma = 4 \times 10^{-9} \text{ mol/cm}^2$ ) electrodes at pH 1.0 (0.1 M  $\text{HClO}_4$ , 0.4 M  $\text{LiClO}_4$ ) at 1.3 V with  $[\text{MTO}] = 4 \text{ mM}$ . Steady-state currents of  $33 \mu\text{A/cm}^2$  and  $15 \mu\text{A/cm}^2$  were obtained for the fully and half loaded films, respectively (Figure S-9). This observation is consistent with a single-site surface mechanism for MTO oxidation. It also rules out rate-limiting diffusion of MTO into the films. By inference, under the conditions of these experiments, rapid diffusion and equilibration of MTO occurs throughout the mesoporous nanostructures.

A possible mechanism for MTO oxidation by nanoITO- $\text{Ru}^{\text{IV}}(\text{OH})_3^{3+}$  is shown in Scheme 1. It features initial  $2e^-/1\text{H}^+$  activation to nanoITO- $\text{Ru}^{\text{IV}}(\text{OH})_3^{3+}$ , followed by a reaction with MTO to give an observable intermediate. Based on the results

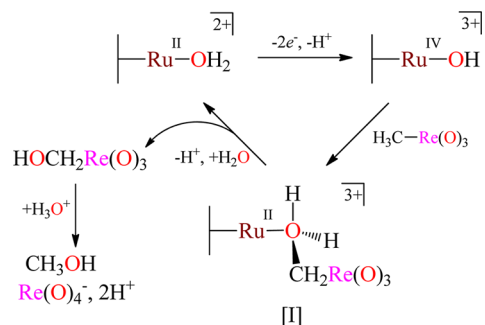
### Scheme 1. Proposed Re–C Insertion Mechanism for MTO Oxidation by nanoITO- $\text{Ru}^{\text{IV}}(\text{OH})_3^{3+}$



of studies on MTO oxidation by oxygen atom-transfer reagents,<sup>6d–j,7</sup> the intermediate may arise from insertion of  $\text{-Ru}^{\text{IV}}(\text{OH})_3^{3+}$  into the Re–C bond of MTO in the initial step. Insertion would give the methanol-bridged, heterobinuclear intermediate,  $[\text{nanoITO-Ru}^{\text{II}}(\mu\text{-O}(\text{H})\text{CH}_3)\text{Re}(\text{O})_3]^{3+}$  (I) shown in Scheme 1. In this mechanism, the catalytic oxidation cycle is completed by hydrolysis of I by 2 equiv of water to give the reduced form of the catalyst, nanoITO- $\text{Ru}^{\text{II}}(\text{OH})_2^{2+}$ , methanol, and perrhenate with release of a proton ( $\text{p}K_{\text{a}}(\text{HReO}_4) = -1.24$ ).

An alternate mechanism with C–H insertion to give a  $\mu_2$  hydroxymethyl-bridged intermediate,  $[\text{nanoITO-Ru}^{\text{II}}(\mu_2\text{-O}(\text{H})_2\text{CH}_2)\text{Re}(\text{O})_3]^{3+}$ , is shown in Scheme 2. Evidence for

### Scheme 2. C–H Bond Insertion Mechanism for MTO Oxidation by nanoITO- $\text{Ru}^{\text{IV}}(\text{OH})_3^{3+}$



related C–H insertion mechanisms has been obtained in the oxidation of benzyl alcohol and alkyl aromatics by nanoITO- $\text{Ru}^{\text{V}}(\text{O})_3^{3+}$ .<sup>8d,f,g</sup> In this mechanism, the overall conversion to methanol is completed by hydrolysis of the intermediate to give nanoITO- $\text{Ru}^{\text{II}}(\text{OH})_2^{2+}$  and  $(\text{HOCH}_2)\text{Re}(\text{O})_3$ , followed by hydrolysis of  $(\text{HOCH}_2)\text{Re}(\text{O})_3$  to give methanol and a perrhenate anion.

An important experimental observation supporting the Re–C bond insertion mechanism in Scheme 1 is the appearance of a well-resolved singlet resonance in the  $^1\text{H}$  NMR spectrum of the methanol product from the CPE experiments in  $\text{D}_2\text{O}$  at pH 1.0 (Figure S-4). If a C–H bond insertion mechanism was operative (Scheme 2), a triplet  $^1\text{H}$  NMR resonance characteristic of  $\text{DH}_2\text{COH}$  as the product would have been observed.

The results described here are significant in providing the first example of an electrocatalytic strategy for oxygen insertion into a metal–carbon bond. There are few chemical examples of this reaction with only one having been shown to be catalytic.<sup>7</sup> The narrow set of potentials for selective oxidation of MTO to

methanol is also notable. Oxidative activation of nanoITO-Ru<sup>II</sup>(OH)<sub>2</sub><sup>2+</sup> in acidic solution provides access to nanoITO-Ru<sup>IV</sup>(OH)<sub>3</sub><sup>3+</sup> (pK<sub>a</sub> ~3). It was previously shown that nanoITO-Ru<sup>IV</sup>(OH)<sub>3</sub><sup>3+</sup> is an electrocatalyst for oxidation of benzyl alcohol.<sup>8f</sup> At 1.3 V, -Ru<sup>IV</sup>(OH)<sub>3</sub><sup>3+</sup> selectively oxidizes MTO to methanol in 87% Faradaic yield. Selectivity is lost at 1.4 and 1.5 V due to overoxidation of MTO by -Ru<sup>V</sup>(O)<sub>3</sub><sup>3+</sup>. The available kinetic and mechanistic information points to a mechanism involving -Ru<sup>IV</sup>(OH)<sub>3</sub><sup>3+</sup> insertion into the Re–C bond of MTO. The reaction proceeds through a detectable intermediate which, at high MTO concentrations, accumulates on the surface undergoing hydrolysis to methanol and perrhenate.

## ■ ASSOCIATED CONTENT

### ■ Supporting Information

Experimental methods, CV and chronoamperometric data, and spectroelectrochemical data are provided. This material is available free of charge via the Internet at <http://pubs.acs.org>.

## ■ AUTHOR INFORMATION

### Corresponding Author

tjmeyer@unc.edu

### Notes

The authors declare no competing financial interest.

## ■ ACKNOWLEDGMENTS

Funding by the Center for Catalytic Hydrocarbon Functionalization, an Energy Frontier Research Center (EFRC), funded by the U.S. Department of Energy (DOE), Office of Science, Office of Basic Energy Sciences, under Award DE-SC0001298 is gratefully acknowledged for supporting M.K.C. and M.A.M. Funding by the UNC EFRC Center for Solar Fuels, an EFRC funded by the U.S. DOE, Office of Science, Office of Basic Energy Sciences, under Award DE-SC0001011 is gratefully acknowledged for supporting J.J.C.

## ■ REFERENCES

- (1) (a) Weissmehl, K.; Arpe, H.-J. *Industrial Organic Chemistry*, 3rd ed.; Wiley-VCH: Weinheim, 1997. (b) Derouane, E. G.; Haber, J.; Lemon, F.; Ribeiro, F.; Guisnet, M. *Catalytic Activation and Functionalization of Light Alkanes – Advances and Challenges*; Kluwer Academic Publishers: Dordrecht, the Netherlands, 1998. (c) Olah, G. A.; Molnár, A. *Hydrocarbon Chemistry*, 2nd ed.; John Wiley and Sons Publishing: Hoboken, NJ, 2003. (d) Wittcoff, H. A.; Reuben, B. G.; Plotkin, J. S. *Industrial Organic Chemicals*, 2nd ed.; John Wiley and Sons Publishing: Hoboken, NJ, 2004.
- (2) (a) Arndtsen, B. A.; Bergman, R. G.; Mobley, T. A.; Peterson, T. H. *Acc. Chem. Res.* **1995**, *28*, 154–162. (b) Stahl, S. S.; Labinger, J. A.; Bercaw, J. E. *Angew. Chem., Int. Ed.* **1998**, *37*, 2180–2192. (c) Crabtree, R. H. *J. Organomet. Chem.* **2004**, *689*, 4083–4091. (d) Labinger, J. A.; Bercaw, J. E. *Nature* **2002**, *417*, 507–514. (e) Hashiguchi, B. G.; Bischof, S. M.; Konnick, M. M.; Periana, R. A. *Acc. Chem. Res.* **2012**, *45*, 885–898.
- (3) (a) Shilov, A. E.; Shul'pin, G. B. *Russ. Chem. Rev.* **1987**, *56*, 442–464. (b) Shilov, A. E.; Shul'pin, G. B. *Chem. Rev.* **1997**, *97*, 2879–2932. (c) Periana, R. A.; Taube, D. J.; Evitt, E. R.; Löffler, D. G.; Wentreck, P. R.; Voss, G.; Masuda, T. *Science* **1993**, *259*, 340–343. (d) Gang, X.; Birch, H.; Zhu, Y.; Hjuler, H. A.; Bjerrum, N. J. *J. Catal.* **2000**, *196*, 287–292. (e) Periana, R. A.; Taube, D. J.; Gamble, S.; Taube, H.; Satoh, T.; Fujii, H. *Science* **1998**, *280*, 560–564. (f) Periana, R. A.; Mironov, O.; Taube, D.; Bhalla, G.; Jones, C. J. *Science* **2003**, *301*, 814–818. (g) Zerella, M.; Mukhopadhyay, S.; Bell, A. T. *Chem. Commun.* **2004**, 1948–1949. (h) Jones, C. J.; Taube, D.; Ziatdinov, V. R.; Periana, R. A.; Nielsen, R. J.; Oxgaard, J.; Goddard, W. A., III

*Angew. Chem., Int. Ed.* **2004**, *117*, 30–32. (i) De Vos, D. E.; Sels, B. F. *Angew. Chem., Int. Ed.* **2005**, *44*, 30–32.

(4) (a) Brown, S. N.; Mayer, J. M. *J. Am. Chem. Soc.* **1996**, *118*, 12119–12133. (b) Bales, B. C.; Brown, P.; Behestani, A.; Mayer, J. M. *J. Am. Chem. Soc.* **2005**, *127*, 2832–2833. (c) Tenn, W. J., III; Young, K. J. H.; Bhalla, G.; Oxgaard, J.; Goddard, W. A., III; Periana, R. A. *J. Am. Chem. Soc.* **2005**, *127*, 14172–14173. (d) Conley, B. L.; Ganesh, S. K.; Gonzales, J. M.; Tenn, W. J., III; Oxgaard, J.; Goddard, W. A., III; Periana, R. A. *J. Am. Chem. Soc.* **2006**, *128*, 9018–9019. (e) Kloek, S. M.; Heinekey, D. M.; Goldberg, K. I. *Angew. Chem., Int. Ed.* **2007**, *46*, 4736–4738. (f) Gonzales, J. M.; Distasio, R., Jr.; Periana, R. A.; Goddard, W. A., III; Oxgaard, J. *J. Am. Chem. Soc.* **2007**, *129*, 15794–15804. (g) Conley, B. L.; Ganesh, S. K.; Gonzales, J. M.; Ess, D. H.; Nielsen, J. R.; Ziatdinov, V. R.; Oxgaard, J.; Goddard, W. A., III; Periana, R. A. *Angew. Chem., Int. Ed.* **2008**, *47*, 7849–7852. (h) Allen, K. E.; Heinekey, D. M.; Goldman, A. S.; Goldberg, K. I. *Organometallics* **2013**, *32*, 1579–1582.

(5) (a) Matsunaga, P. T.; Mavropoulou, J. C.; Hillhouse, G. L. *Polyhedron* **1995**, *14*, 175–185. (b) Koo, K.; Hillhouse, G. L.; Rheingold, A. L. *Organometallics* **1995**, *14*, 456–460.

(6) (a) Abu-Omar, M. M.; Hansen, P. J.; Espenson, J. H. *J. Am. Chem. Soc.* **1996**, *118*, 4966–4974. (b) Espenson, J. H.; Tan, H.; Mollah, S.; Houk, R. S.; Eager, M. K. *Inorg. Chem.* **1998**, *37*, 4621–4624. (c) Copéret, C.; Adolfsson, H.; Khuong, T.-A. V.; Yudin, A. K.; Sharpless, K. B. *J. Org. Chem.* **1998**, *63*, 1740–1741. (d) Gonzales, J. M.; Diastro, R., Jr.; Periana, R. A.; Goddard, W. A., III; Oxgaard, J. *J. Am. Chem. Soc.* **2007**, *129*, 15794–15804. (e) Bischof, S. M.; Cheng, M.-J.; Nielsen, R. J.; Gunnoe, T. B.; Goddard, W. A., III *Organometallics* **2011**, *30*, 2079–2082. (f) Figg, T. M.; Cundari, T. R.; Gunnoe, T. B. *Organometallics* **2011**, *30*, 3779–3785. (g) Figg, T. M.; Webb, J. R.; Cundari, T. R.; Gunnoe, T. B. *J. Am. Chem. Soc.* **2012**, *134*, 2332–2339. (h) Cheng, M.-J.; Bischof, S. M.; Nielsen, R. J.; Goddard, W. A., III; Gunnoe, T. B.; Periana, R. A. *Dalton Trans.* **2012**, *41*, 3758–3763. (i) Mei, J.; Carsch, K. M.; Freitag, C. R.; Gunnoe, T. B.; Cundari, T. R. *J. Am. Chem. Soc.* **2013**, *135*, 424–435. (j) Pardue, D. B.; Mei, J.; Cundari, T. R.; Gunnoe, T. B. *Inorg. Chem.* **2014**, *53*, 2968–2975.

(7) Pouy, M. J.; Milczek, E. M.; Figg, T. M.; Otten, B. M.; Prince, B. M.; Gunnoe, T. B.; Cundari, T. R.; Groves, J. T. *J. Am. Chem. Soc.* **2012**, *134*, 12920–12923.

(8) (a) Concepcion, J. J.; Jurss, J. W.; Templeton, J. L.; Meyer, T. J. *J. Am. Chem. Soc.* **2009**, *130*, 16462–16463. (b) Concepcion, J. J.; Tsai, M.-K.; Muckerman, J. T.; Meyer, T. J. *J. Am. Chem. Soc.* **2010**, *132*, 1545–1557. (c) Chen, Z.; Concepcion, J. J.; Hu, X.; Yang, W.; Hoertz, P. G.; Meyer, T. J. *Proc. Natl. Acad. Sci. U.S.A.* **2010**, *107*, 7225–7229. (d) Paul, A.; Hull, J. F.; Norris, M. R.; Chen, Z.; Ess, D. H.; Concepcion, J. J.; Meyer, T. J. *Inorg. Chem.* **2011**, *50*, 1167–1169. (e) Chen, Z.; Vannucci, A. K.; Concepcion, J. J.; Jurss, J. W.; Meyer, T. J. *Proc. Natl. Acad. Sci. U.S.A.* **2011**, *108*, 1461–1469. (f) Vannucci, A. K.; Hull, J. F.; Chen, Z.; Binstead, R. A.; Concepcion, J. J.; Meyer, T. J. *J. Am. Chem. Soc.* **2012**, *134*, 3972–3975. (g) Vannucci, A. K.; Chen, Z.; Concepcion, J. J.; Meyer, T. J. *ACS Catal.* **2012**, *2*, 716–719.

(9) (a) Chen, Z.; Concepcion, J. J.; Jurss, J. W.; Meyer, T. J. *J. Am. Chem. Soc.* **2009**, *131*, 15580–15581. (b) Gagliardi, C. J.; Vannucci, A. K.; Concepcion, J. J.; Chen, Z.; Meyer, T. J. *Energy Environ. Sci.* **2012**, *5*, 7704–7717.

(10) Bard, A. J.; Faulkner, L. R. *Electrochemical Methods, Fundamentals and Applications*, 2nd ed.; John Wiley and Sons: Hoboken, NJ, 2004.

(11) (a) Carey, F. A.; Sundberg, R. J. *Advanced Organic Chemistry, Part A: Structure and Mechanisms*, 4th ed.; Springer Science+ Business Media, LLC: New York, 2006. (b) Kim, S.-J.; Choi, D.-W.; Lee, Y.-J.; Chae, B.-H.; Ko, J.; Kang, S. O. *Organometallics* **2004**, *23*, 559–567.